Dynamics of Firefly Luciferase Inhibition by General Anesthetics: Gaussian and Anisotropic Network Analyses

Agnieszka Szarecka,* Yan Xu,*† and Pei Tang*†‡
Departments of *Anesthesiology, †Pharmacology, and ‡Computational Biology, University of Pittsburgh School of Medicine, Pittsburgh, Pennsylvania 15261

ABSTRACT The new crystal structures of the product-bound firefly luciferase combined with the previously determined substrate-free structures allow for a detailed analysis of the dynamics basis for the luciferase enzymatic activities. Using the Gaussian network model and the anisotropic network model, we show here that the superposition of the three slowest anisotropic network model modes, consisting of the bending, rotating, and rocking motions of the C-domain, accounts for large rearrangement of domains from the substrate-free (open) to product-bound (closed) conformation and thus constitutes a critical component of the enzyme's functions. The analysis also offers a unique platform to reexamine the molecular mechanism of the anesthetic inhibition of the firefly luciferase. Through perturbing the protein backbone network by introducing additional nodes to represent anesthetics, we found that the presence of two representative anesthetics, halothane and *n*-decanol, in different regions of luciferase had distinctively different effects on the protein's global motion. Only at the interface of the C- and N-domains did the anesthetics cause the most profound reduction in the overall flexibility of the C-domain and the concomitant increase in the flexibility of the loop, where the substitution of a conserved lysine residue was found experimentally to lead to >2–3 orders of magnitude reduction in activity. These anesthetic-induced dynamics changes can alter the normal function of the protein, appearing as an epiphenomenon of an "inhibition". The implication of the study is that a leading element for general anesthetic action on proteins is to disrupt the modes of motion essential to protein functions.

INTRODUCTION

Firefly bioluminescence, which converts chemical energy from luciferin, Mg-ATP, and oxygen into light, is catalyzed by the enzyme luciferase. This protein belongs to the superfamily of acyl-adenylate-forming and thioester-forming enzymes, which have been subjected to intense structural investigations in recent years (1–6). These enzymes are believed to adopt two different conformations to catalyze two half reactions (4): the first half is an adenylation reaction to form an acyl-adenylate from a carboxylate and ATP, and the second half is either an oxidative decarboxylation in the case of luciferase or an acyl-group-transfer reaction in other members. More generally, the proteins in this superfamily can act as a multifunctional enzyme—both as oxygenase and ligase (7,8)—and their activity depends strongly on the concentrations of native substrates as well as the presence of coenzyme A. The modes of motion to accomplish the large domain rearrangement, which is essential for function, are yet to be elucidated.

In a seemingly completely unrelated field, luciferase has also been the focus of the debate on molecular mechanisms of general anesthesia, a topic that has far-reaching implications for the physiology of consciousness, arousal and sleep, and memory formation. It was discovered quite unexpectedly some 40 years ago that the bioluminescence activity of luciferase could be inhibited by general anesthetics (9). This intriguing finding (9), along with a more systematic investigation two decades later with anesthetics over a potency range of five orders of magnitude (10), directly challenged the century-long dominance of the lipid theory of general anesthesia and brought the protein theory onto the center stage. The inhibition of luciferase by anesthetics provided convincing evidence, showing direct anesthetic interaction with proteins to exert an action. What remains elusive is how protein functions are modulated by anesthetics. The suggestion—based on the studies with luciferase—that anesthetics might "act by competing with endogenous ligands for binding to specific receptors" (10) and the inference that they might "act at a relatively small number of sensitive protein targets" (11) has led the mainstream anesthesia research onto a path of searching for specific and perhaps discrete anesthetic-sensitive binding sites in the central nervous system. The past 20 years have witnessed much excitement (12) and disappointment along with a few misinterpretations or overinterpretations of experimental results at the molecular, cellular, and systemic levels. Even with isolated proteins like luciferase, the interpretations of how anesthetic molecules affect protein functions are controversial (2,13–16).

Although hydrophobic pockets allowing some anesthetic (or even nonanesthetic) binding undoubtedly exist in proteins, a protein theory based simply on structural fitting to the yet unidentified protein targets by anesthetic molecules, which range from the noble gas xenon to complex steroids, seems inadequate in explaining and predicting the action of these drugs. We have proposed an alternative viewpoint of

Submitted December 7, 2006, and accepted for publication May 10, 2007.

Address reprint requests to Prof. Pei Tang, PhD, 2049 Biomedical Science Tower 3, 3501 Fifth Ave., University of Pittsburgh, Pittsburgh, PA 15260. Tel.: 412-383-9798; Fax: 412-648-8998; E-mail: tangp@anes.upmc.edu.

Editor: Ivet Bahar.

0006-3495/07/09/1895/11 $2.00

doi: 10.1529/biophysj.106.102780

anesthetic action based on protein global dynamics (17). This dynamics-function paradigm can potentially unify the action of a diverse range of anesthetics on a given protein based on their ability to modulate the functional mobility of the protein. We contend that the primary action of general anesthetics (and possibly other low-affinity drugs) on proteins is to disrupt the modes of motion essential to protein function. Binding to structurally fitting pockets is often sufficient but not necessary.

Perhaps the most appropriate protein model to test our hypothesis is again the luciferase, given its susceptibility to modulations by a diverse range of anesthetics at their respective clinical concentrations. The recent advent of the high-resolution x-ray structures of the product-bound (adenosine 5′-monophosphate (AMP) and oxyluciferine) luciferase from the Japanese *Genji-botaru* (6), combined with the previously determined structures of the substrate-free luciferase from the American firefly *Photinus pyralis* (2,18), provides the structural basis for understanding the activities of luciferase. These two species of the enzyme are highly homologous and have 67% sequence identity and >80% sequence similarity. Therefore, their structures, representing two different functional states of luciferase, make a good pair in this study for us to characterize the intrinsic dynamics of the enzyme, to delineate the essential link between dynamics and function of luciferase, and to reveal the susceptibility of protein motions to anesthetic modulations.

Like other members in the superfamily, luciferase has a large N-terminal domain (residues 1–436 in the *Photinus pyralis* sequence) and a small C-terminal domain (residues 440–550) connected through a short hinge. Fig. 1 depicts the experimental structures of luciferase in substrate-free and product-bound states along with the naming of the most prominent domains and subdomains. The substrate-free structure represents an ''open'' conformation with a large solvent-exposed cleft between the N- and C-domains (Fig. 1 *A*). In contrast, the product-bound structure demonstrates a ''closed'' conformation (Fig. 1 *B*). The transition from the open to the closed conformation seems to involve a rigid-body bending of C-domain toward the N-domain and a ~90° counterclockwise rotation of the C-domain relative to the N-domain. Most of the substrate binding residues determined experimentally, notably by mutagenesis, are located in the N-terminal domain forming a cavity in the core of the domain, with an open access pathway at the cleft. As shown in Fig. 1 *B*, luciferin binds at the bottom of the pocket and ATP above it, closer to the domain interface and the cleft.

The N-terminal domain harbors the L1 loop (residues 198–206), which is a signature sequence in the superfamily (1,18). Although the N-terminal domain has by itself a certain unassisted capacity to sustain the biological function of the enzyme (19), the role of the C-domain is believed to be absolutely essential for efficiency and catalytic yield. The Lys^{529} residue in loop L2 (residues 524–533, Fig. 1 *A*) of the C-terminal domain has been shown to play a crucial role in orienting the substrates (20). Most interestingly, all the invariant residues in the superfamily are located on the cleft-facing surfaces of both domains or in the hinge-linker segment. A diverse range of tertiary relationships between the N- and C-domains has also been found in the x-ray crystal structures of other luciferase-related proteins (1,3–5), suggesting that the C-domain of these proteins is intrinsically mobile and its movement relative to the N-domain is essential for these proteins to carry out their biological functions.

To accurately capture the essential backbone global dynamics and low-frequency modes of motion relevant to protein functions, coarse-grained simulation is often sufficient. Recent developments based on the elastic network normal mode analysis (21,22) conclude that a detailed description of specific interresidue interactions is not necessary to correctly characterize the low-frequency motions. Further reduction of the system complexity by adopting the one-point-per-residue (usually C_α atom) scheme, such as in the Gaussian network model (GNM) (23) and anisotropic network model (ANM) (24), has been shown to successfully capture a wide range of protein dynamics (25,26). In this

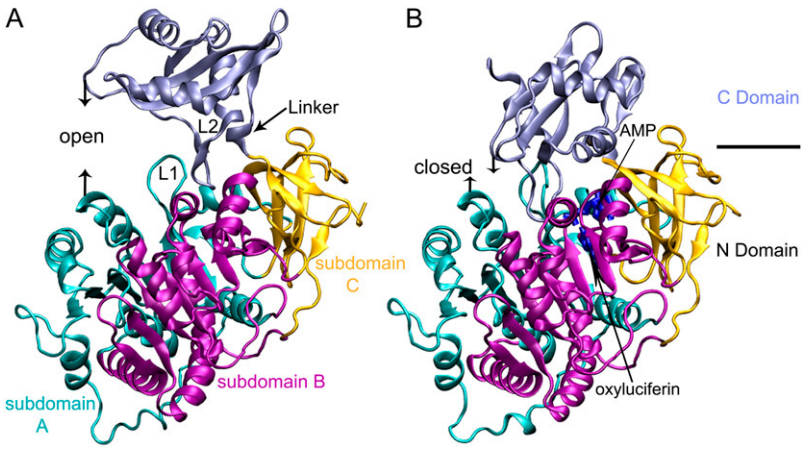

FIGURE 1 Firefly luciferase in (*A*) an open substrate-free conformation (PDB: 1BA3) with a large cleft separating the C- and N-terminal domains; and (*B*) a closed substrate-bound conformation (PDB: 2D1R), where the C-domain is much closer to the N-domain. The reaction products, AMP and oxyluciferin, are marked in blue. The subdomains in the N-domain are highlighted in cyan, purple, and yellow and labeled accordingly along with three highly conserved loops. Notice that the primary difference between the open and closed conformation is the C-domain arrangement relative to the N-domain.

study, we used GNM and ANM to analyze luciferase's dynamical features that have direct consequences on the enzymatic activities. On the basis of this analysis, we have also carried out systematic computational anesthetic docking using two representative general anesthetics, halothane and *n*-decanol, to examine the potential anesthetic interaction sites in luciferase. Furthermore, we elucidated and quantified the specific anesthetic effects on the global dynamics of luciferase using GNM and ANM. Taken together, our computations on luciferase provided new insights into the mechanism of anesthetic inhibition of luciferase enzymatic activities.

MATERIALS AND METHODS

X-ray structures of luciferase

The x-ray structures of luciferase in the apo form (18), in the substrate-free conformation but with two bromoform molecules (2), and in the product-bound conformation (6) were obtained from the Protein Data Bank (PDB codes: 1LCI, 1BA3, and 2D1R, respectively). Of over 500 residues in luciferase, only two residues (199 and 200) are unresolved in 1BA3. These two missing residues were reconstructed using the MODLOOP server (27) and further energy minimized using the NAMD program (28). All of the residues in the 2D1R structure are well resolved. In 1LCI, however, many residues are unresolved in four highly disordered regions. Comparing the resolved part of 1LCI to 1BA3, the root mean-square deviation (RMSD) between the two is very small (<1 Å), consistent with the fact that 1BA3 was obtained by simply soaking the apoluciferase crystal transiently in a saturated bromoform solution (2). Therefore, the high-resolution structures of 1BA3 and 2D1R were chosen in this study to represent luciferase conformations without and with native substrates, respectively.

GNM and ANM

The theoretical description of the GNM and ANM has been detailed previously (24,29,30). Briefly, both models assume that a protein in its folded state can be represented by a three-dimensional elastic network of N nodes placed on C_α atoms (N = the number of residues in the protein). The pairs of nodes within a cutoff radius of R_c (6.0 and 15 Å for GNM and ANM, respectively), irrespective of whether bonded or nonbonded, are assumed to be connected by springs with a uniform force constant, γ. In GNM (29), the $N \times N$ Kirchhoff matrix defines the topology of interresidue contacts. The mean-square fluctuations of residue ($i = j$) or their cross correlations ($i \neq j$) can be expressed as

$$\langle \Delta \mathbf{R}_i \Delta \mathbf{R}_j \rangle = \frac{3k_B T}{\gamma} [\mathbf{\Gamma}^{-1}]_{ij}, \quad (1)$$

where $\mathbf{\Gamma}$ is the Kirchhoff matrix, k_B the Boltzmann constant, T the absolute temperature, and γ the force constant. It is worth mentioning that the γ values do not affect the calculated motional pattern but only the overall scaling of the amplitude of fluctuation along the protein sequence. In this study, the γ values were determined by reproducing the experimental B factors of the crystal structures. The beauty of GNM is the possibility to extract the global motion of a large protein with minimum computational cost. The dynamic spectrum of a protein can be quickly decomposed with the GNM analysis into a set of normal modes in which the first several slow modes are usually associated with the functionally relevant motions (25,26, 31,32). However, GNM provides information only on the relative magnitude of fluctuations. The directionality of the motions can be characterized by ANM (24), in which the counterpart of the Kirchhoff matrix $\mathbf{\Gamma}$ in GNM is the $3N \times 3N$ Hessian matrix, $\mathbf{H}$. ANM decomposes the motion spectrum of a protein into $3N - 6$ nonzero eigenvalues and the same number of eigenvectors that reveal the respective frequencies and shapes of individual modes. The inverse of Hessian matrix, $\mathbf{H^{-1}}$, is composed of $N \times N$ superelements, and the ith superelement of $\mathbf{H^{-1}}$ describes the self-correlations between the components of $\Delta \mathbf{R}_i$. Protein conformational changes induced by a given mode, k, can be evaluated using the ANM-predicted eigenvector $\boldsymbol{\mu}_k^{ANM}$as in (33):

$$[\mathbf{R}(\pm s)]_k = \mathbf{R}^0 \pm s_k \lambda_k^{-1/2} \boldsymbol{\mu}_k^{ANM}, \quad (2)$$

where $\mathbf{R}^0$ and $\mathbf{R}$ are the vectors of the original and instantaneous C_α positions, respectively, λ_k is the eigenvalue, and s_k is the scaling parameter that scales the size of deformation induced by mode k. The formula was employed to demonstrate the open-to-closed transition of luciferase in this study.

The software for GNM and ANM calculations was obtained from http://ribosome.bb.iastate.edu/software.html, and the calculations were run on Dell Precision 530 workstations equipped with dual Xeon processors. The online servers developed in the Bahar laboratory (http://ignm.ccbb.pitt.edu/GNM_Online_Calculation.htm (34,35) and http://ignmtest.ccbb.pitt.edu/cgi-bin/anm/anm1.cgi) were also used for part of the calculations.

Anesthetic docking

Potential anesthetic interaction sites in luciferase were explored by docking anesthetic halothane and *n*-decanol to the substrate-free and product-bound luciferase using the AutoDock3.0 program (36). The previously optimized parameter set for halothane (37,38) was used in halothane docking. The initial structure of *n*-decanol was obtained from geometry optimization at the quantum mechanical B3LYP/6-311(G) level of theory using the Gaussian98 suite of programs (39). Default parameters from AutoDock3.0 were adopted for *n*-decanol docking. Torsion-angle flexibility was allowed for *n*-decanol and halothane molecules. A grid size of 164, 180, and 156 in the X, Y, and Z dimensions with a spacing resolution of 0.436 Å was used in docking. Other docking conditions, including the Lamarckian genetic algorithm, are the same as used in our previous studies (40). Favorable docking results were determined on the basis of low docking energy and high occupancy. At least 100 docking trials were performed for each system with different configurations of substrate or product binding.

Analysis of anesthetic effects on protein global dynamics

The nodes representing anesthetic molecules were placed on selected carbon atoms in GNM calculations. For halothane, a single node was placed on the CF_3 carbon atom. For *n*-decanol, to achieve the coarse-graining level similar to that for the protein network, every three carbons were represented by one node, resulting in four nodes per *n*-decanol molecule. To verify the robustness of our results with respect to the coarse graining of the anesthetic molecules, we also carried out calculations with three or six nodes per *n*-decanol molecule and proved that the choice of three, four, or six nodes per *n*-decanol did not affect the conclusion. No distinction was made for interaction potentials between protein and nonprotein nodes. Such an approximation is reasonable in GNM calculations, where a uniform force constant was applied to all nodes in the network.

The mean-square fluctuation driven by the global GNM modes of luciferase in the presence of anesthetics, $\langle \Delta \mathbf{R}^2 \rangle_{(\text{protein+anesthetics})}$, was compared with the results from parallel calculations without anesthetics. Anesthetic-induced dynamics changes were determined using the differences in the root mean-square fluctuations (RMSF) of luciferase in the presence and absence of anesthetics, $(\text{sqrt}\langle \Delta \mathbf{R}^2 \rangle_{(\text{protein+anesthetics})} - \text{sqrt}\langle \Delta \mathbf{R}^2 \rangle_{(\text{protein})})$.

RESULTS AND DISCUSSION

Links between dynamics and function

The lowest frequency GNM and ANM modes of luciferase exhibit the characteristics of concerted motions that coincide strikingly well with the experimental findings. The RMSF, derived from the slowest GNM mode, were color coded onto the original open and closed structures of luciferase in Fig. 2, showing that the C-domain is actively engaged in motion whereas the N-domain is much less involved. The correctness of the GNM result is clearly evidenced by the substantial changes in the C-domain orientation in the structures of substrate-free and product-bound luciferase, whereas the N-domain conformation remains almost the same with and without substrate binding.

The highly dynamical nature of the C-domain is reflected not only in the large amplitude of domain fluctuations in the GNM global mode but also in the directions of domain motions as revealed by the ANM analyses. In Fig. 3, *A–E*, we present four conformational models generated using Eq. 2 by displacing C_α in the open structure along the eigenvectors of the three slowest ANM modes. The conformational transition from the open to the closed conformation requires a large amplitude movement of the C domain (see Fig. 3 *A*) with a downward movement by ~5 Å and lateral rotation of ~90°. The C_α RMSD between the open and closed conformations is >17 Å for the C domain when the two structures are fitted by the N-domain. Because harmonic approximations near the equilibrium structure are used in the ANM analysis, the large displacement of this magnitude, which is beyond the harmonic regime, will undoubtedly introduce distortions into the secondary structure. Thus, in determining the scaling factors s_k in Eq. 2, we limited s_k values to not exceed 65, with signs producing the ''correct'' direction of movement toward the closed structure. The s_k values for the first three modes were optimized iteratively to minimize the C_α RMSD of the C-domain between the transformed structure from Eq. 2 and the experimental closed structure. The optimized s_k values for the first three modes are 9, −37, and −3, respectively, and were used to generate Fig. 3, *B–D*, discussed below. The superposition of these three modes of motion is shown in Fig. 3 *E*, which reduces the C_α RMSD of the C-domain from 17 Å to 11 Å. It is important to emphasize that the ANM eigenvectors cannot reproduce the complete conformational transition but rather can only identify the modes of motions that correlate closely with the directions and the tendency of the functionally important conformational changes.

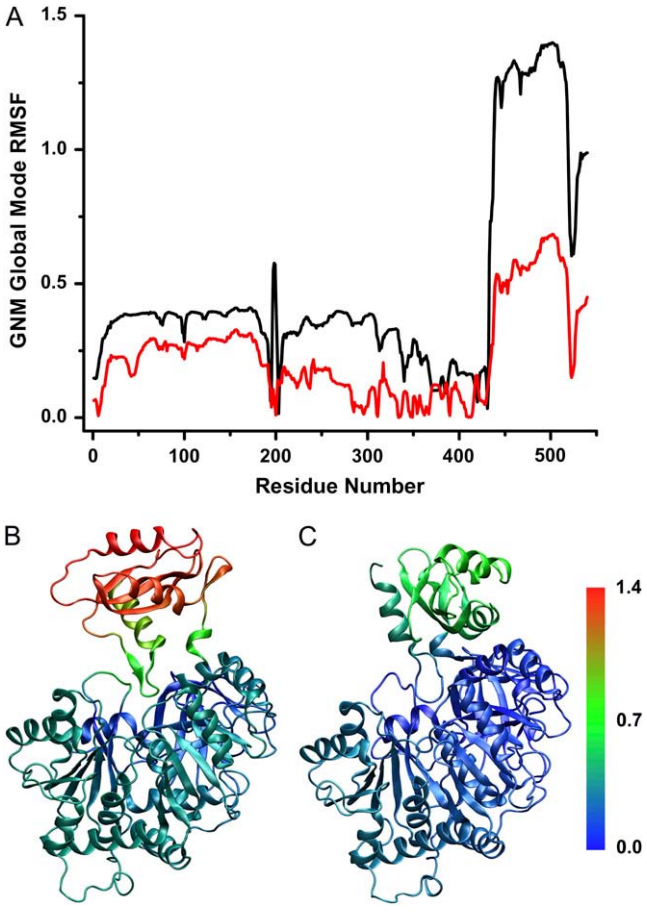

FIGURE 2 (*A*) RMSF driven by the GNM global (first) mode in the open (*black*) and closed (*red*) conformations of firefly luciferase. The RMSF values are mapped onto the (*B*) open and (*C*) closed conformations of luciferase. The low amplitude of N-domain fluctuations (largely in *blue*) is in sharp contrast to the high mobility of those of the C-domain (largely in *red* and *green*).

The first ANM mode of the substrate-free luciferase drives a downward hinge-bending, cleft-closing movement of the C-domain (Fig. 3 *B*). It has been postulated that the motion of the small C-domain toward the large N-domain in a ''hammer-and-anvil'' fashion (41) is induced by ATP binding and allows all the invariant residues, which are located in the linker and on the cleft-facing surfaces of the two domains, to move closer to interact with the substrate. The second slowest ANM mode drives rotation of the C-domain with respect to the N-domain, coupled with a slight tilting of the N-domain in the opposite direction (Fig. 3 *C*). A rocking motion is revealed in the third ANM mode (Fig. 3 *D*). The superposition of the bending, rotating, and rocking motions results in a conformation, as shown in Fig. 3 *E*, which constitutes a transition stage toward the closed conformation of luciferase (Fig. 1 *B*) and other homologous proteins crystallized in the ''catalytic'' states (1). Clearly, the transition between the open and closed conformations, which respond to the disassociation and association of substrates, respectively, is realized through a hinged, rigid-body movement involving predominately the C-domain. Such large amplitude movement of the C-domain, consequently leading to a very different tertiary arrangement, has been hypothesized to be essential for accommodating the catalytic reactions by the enzymes in the adenylate-forming superfamily (5).

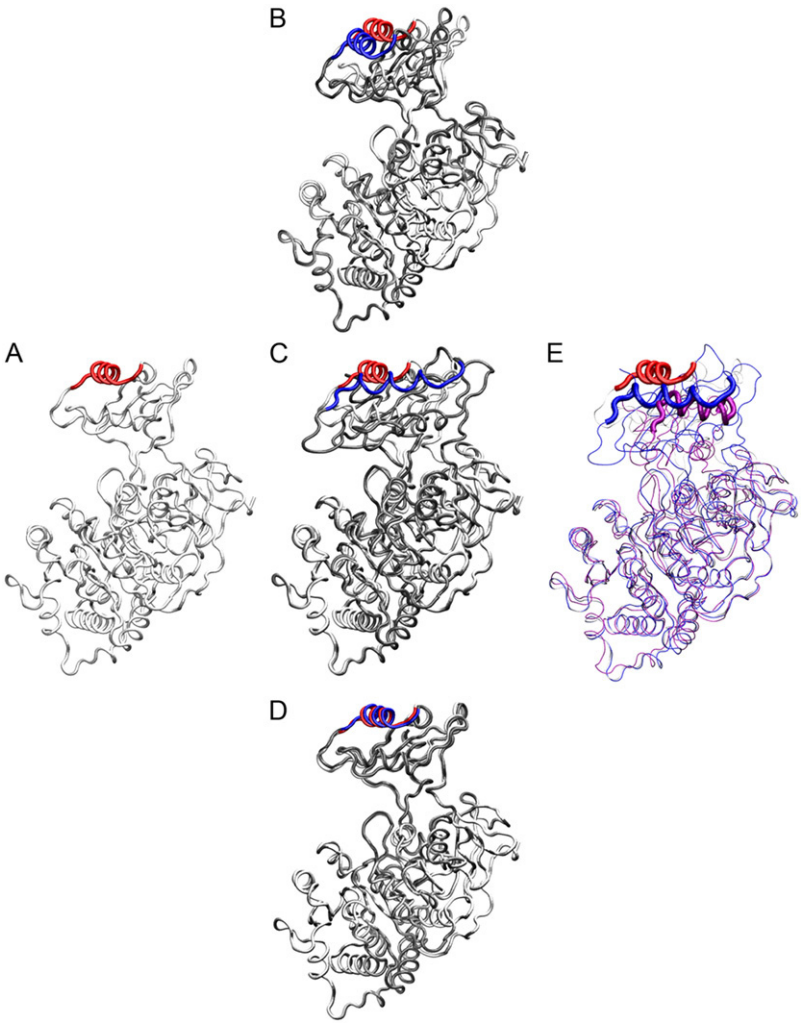

FIGURE 3 Directionality of conformation transition from the open to closed structures of luciferase, predicted by the eigenvectors of the three slowest ANM modes ($k = 1, 2, 3$) using Eq. 2. Note that the N-domain is mostly immobile, whereas the small domain undergoes large-amplitude displacement during the open-to-closed transition. A helix of the C-domain is highlighted in different colors to help visualize the conformational transitions. (*A*) The original open structure (*light gray* with the *red* helix); (*B*) the original open structure superimposed with a model (*dark gray* with the *blue* helix) resulting from a deformation of the open conformation along the slowest mode eigenvector that corresponds to the C-domain downward bending; (*C*) the model structure (*dark gray* with the *blue* helix) resulted from the original open structure through a deformation along the second slowest mode eigenvector that drives the lateral rotation of C-domain; (*D*) the model (*dark gray* with *blue* helix) resulted from the open structure deformed along the third slowest mode eigenvector, the motion of which can be best described as C-domain rocking laterally between subdomains A and B of N-domain; and (*E*) the final model structure (*blue* with the thickened *blue* helix) resulted from the original open conformation through a deformation by the superposition of all three slowest eigenvectors. The model is superimposed with the open (*light gray* with *red* helix) and the closed (*purple* with the *thickened purple* helix) conformations. The scaling factors, s_k, are 9, −37, and −3 for *B*, *C*, and *D*, respectively. The same s_k parameters were applied for the model in *E*. Note that the combined motion yields a conformation that correlates well with the conformational change leading to the experimental crystal structure in the closed form.

Besides the aforementioned rigid body movement of the C-domain that dominates luciferase's global dynamics, other motions may also contribute to the enzymatic activity. To analyze the intrinsic coupling among various residues between the N- and C-domains or among the subdomains, the interresidue cross correlation of motions in all GNM modes is mapped in Fig. 4, displaying several important dynamic features. First, the long-range interactions between N- and C-domains are mainly characterized by a strong and negative correlation. This is more so in the open conformation, whereas added contact points between the N- and C-domains in the closed conformation moderately reduce the negative correlation between the two domains. Second, the C-domain is strongly correlated within itself whereas the N-domain, which contains substrate binding sites, is more diverse in its internal correlations. Third, loops L1 (residues 198–206) and L2 (residues 524–533) constitute the prominent gaps in the anticorrelation between C- and N-domains, and their motions are strongly coupled with each other. This coupling is vividly displayed in Fig. 2, *A* and *B*, in the global mode of the open conformation, where the tips of the L1 and L2 loops are ''locked'' into each other with almost identical RMSF whereas the ''upper'' part of the L2 loop is quite flexible. The coupling provides the functionally important dynamical ''contact'' between the two domains across the cleft. These features are clearly visible in Fig. 4 in both the substrate-free and product-bound conformations, though some appear stronger in one conformation than the other.

To highlight the diverse range of motional correlation within and among the subdomains, higher GNM modes of motion are depicted in Fig. 5. Compared to the global mode (Fig. 2), the collectivity of the higher modes within the N-domain is significantly reduced. In modes 2–5, the flexibility distributions in the N-domain are quite similar for both conformations. The strongly fluctuating segments of the A, B, and C subdomains (see Fig. 1 for subdomain naming) are consistently those that are external and solvent exposed.

The cleft between the N- and C-domain is crucial for luciferase function, and many residues in this region are either invariant or highly homologous in the superfamily

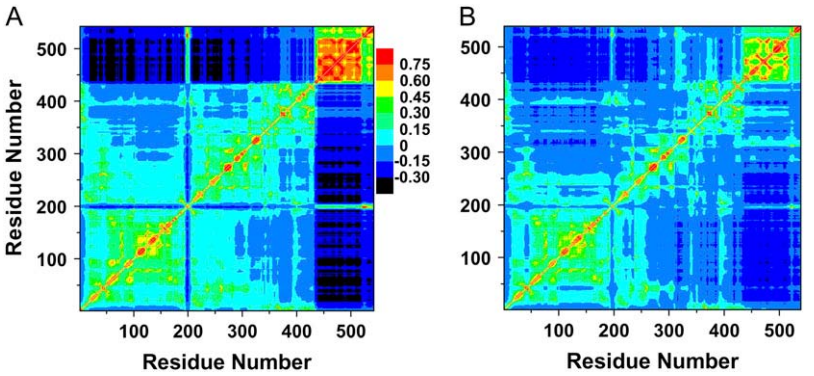

FIGURE 4 Cross correlation of all GNM modes of firefly luciferase in the (*A*) open and (*B*) closed conformations. Strong positive correlations among residues within the C-domain indicate a significant component of collective rigid-body movements of the C-domain. Strong coupling between L1 (residues 198–206) and L2 (524–533) loops and anticorrelation between the N-domain and C-domain are clearly visible.

(18). Some of the residues at the cleft were implicated in directing the substrates into the correct position and orientation (20), interacting with the diffusing products, or facilitating different stages of catalytic pathway (18). Loop L1, containing the superfamily signature sequence, has a very low mobility in the two slowest modes. However, a relatively high flexibility of L1 and L2 is observed in the substrate-free luciferase in GNM modes 3 and 4. The enhanced flexibility of both cleft-projecting loops L1 and L2 may promote the reception and accommodation of substrate molecules in the open conformation. In contrast, these loops remain rigid in most of the slowest modes in the closed form. The rigidity of the loops may assist the stabilization of the productive domain arrangement for acyl-adenylate formation and ultimately facilitate catalysis and light emission. Taken together, GNM and ANM calculations captured the essential dynamics features of luciferase that have direct implication on the function of the protein. These features provide us with the basis for elucidating potential anesthetic effects on luciferase enzymatic activity, as presented below.

Anesthetic interaction sites in luciferase

It has been well documented that the anesthetic modulation of luciferase activity and the nature of anesthetic interaction with the enzyme are strongly dependent on the concentration of Mg-ATP (14,42). At low Mg-ATP concentrations, anesthetics have little inhibitory effects on luciferase activity, suggesting that certain conformational changes upon ATP binding are required for anesthetics to exert their action. For a long time, the site at which anesthetics interact with the enzyme to cause inhibition has remained uncertain. Cocrystallization of luciferase with native substrates or with anesthetics has proven to be rather difficult (2). The only crystal structure of luciferase with two bromoform molecules but without substrates was obtained by soaking the crystals in

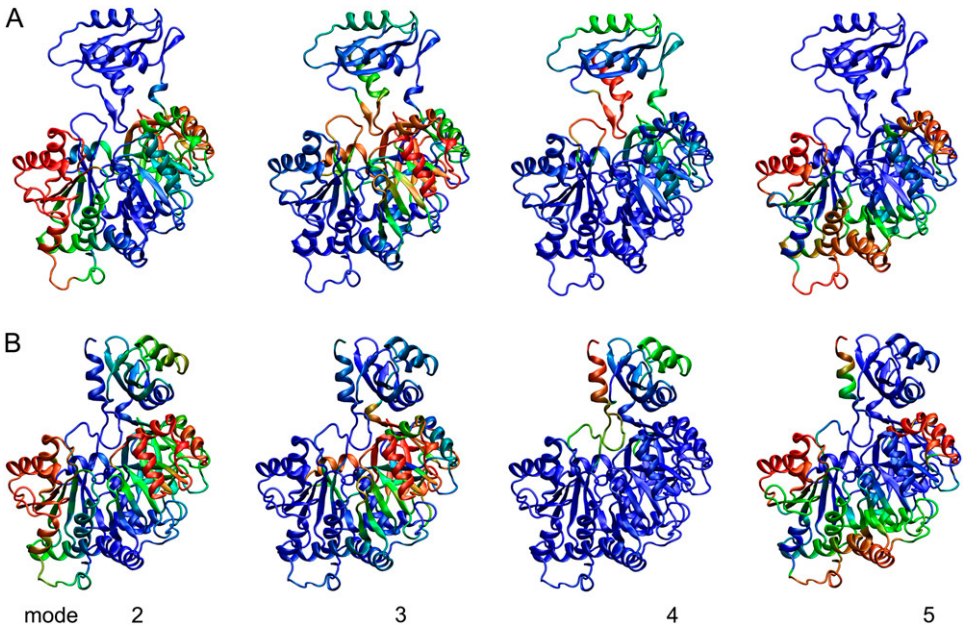

FIGURE 5 MSF driven by GNM modes 2–5 are color mapped onto the (*A*) open and (*B*) closed conformations of the firefly luciferase. Notice the loss of motional collectivity in the N-domain of both conformations. Modes 3 and 4 exhibit significant mobility in loops L1 and L2 of the open form but not in the closed form.

the apo form into saturated bromoform (2). Hence, the relevance of the bromoform site found in the soaked crystal to the real anesthetic inhibition site has to be taken with caution, and other vital binding sites may remain unidentified.

To examine plausible anesthetic interaction sites, we performed flexible anesthetic docking on both luciferase conformations. Halothane and *n*-decanol were chosen for the study because of their difference in size and the inhibition potency. The potency of *n*-decanol is several orders of magnitude stronger than that of halothane (10). At least two conclusions can be drawn from the docking study. First, the distributions of anesthetics in the open and closed forms are different. As shown in Fig. 6, the cleft region of the closed luciferase is more energetically favorable for *n*-decanol. In comparison, the open form harbors the highest affinity site in the A subdomain of the N domain. Second, the product-binding pocket seems to attract anesthetics in both conformations. *N*-decanol docks to the AMP and oxyluciferin binding sites in the closed form when the products in the structure were artificially removed. There was also a certain degree of *n*-decanol affinity for the same cavity in the open form, although it is not the most favorite docking site. Another site with lower affinity in the closed form is in the groove separating subdomains B and C (denoted ''side''). Halothane has similar binding profiles with significant populations in all aforementioned sites. Among them, the most populated site in the open conformation is again located in subdomain A. Other docking sites, including some scattered peripheral sites, are with higher docking energy and lower affinities, consistent with the experimental finding that halothane has much lower inhibition potency to luciferase than *n*-decanol. Detailed anesthetic docking energy and site occupancy are summarized in Table 1S in the Supplementary Material.

We hope that our computational predictions of the multiple low-affinity anesthetic binding sites will prompt further experimental studies on the enzyme and its interactions with volatile anesthetics. Experimental measurements of low-affinity binding with site specificity prove to be extremely difficult because most experimental approaches based on the Scatchard method can only yield the apparent binding constant, which in the case of multiple low-affinity binding sites is heavily skewed toward the comparatively higher affinity sites. Cocrystallization with low-affinity drugs is rarely successful, and even when well-diffracting crystals are obtained,

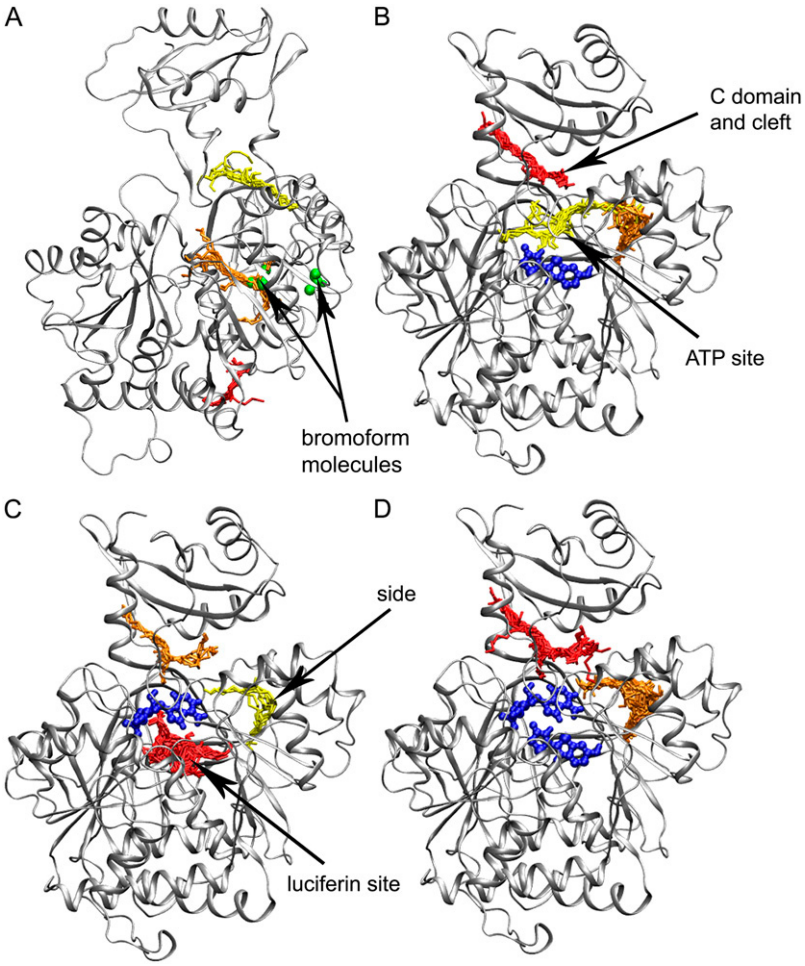

FIGURE 6 Results of *n*-decanol flexible docking in (*A*) the open form of luciferase, (*B*) the closed form with bound oxyluciferin, (*C*) the closed form with bound AMP, and (*D*) the closed form with bound AMP and oxyluciferin. Bromoform locations found in 1BA3 are marked by green spheres in *A*. Both AMP and oxyluciferin are colored in dark blue in *B–D*. Major docked *n*-decanol clusters are displayed with different color codes for binding energies: red, the lowest energy; orange, moderate; and yellow, the high energy. The *n*-decanol docking locations are marked in *B–D* by their proximity to the functionally important sites.

it is often unclear if all possible sites are occupied in the cocrystals. However, with strategic selective isotopic labeling of the backbone and side chains, it is possible in principle to measure the site-specific binding constants by NMR chemical shift perturbation through anesthetic titrations. We have used this method to measure the halothane binding to a small soluble protein, ketosteroid isomerase (D. Ma, Y. Xu, and P. Tang, unpublished data), and confirmed the anesthetic binding at the sites predicted by our computational studies (40). Alternatively, with the availability of an increasing number of synthetic anesthetic agents having photoaffinity probes, it is also possible to explore anesthetic binding by photoaffinity labeling. This method has been successfully applied (43) using [^{14}C] halothane to some anesthetic targets, both in soluble and membrane proteins. Indirectly, the firefly luciferase activity and interaction with anesthetics can be further studied using point mutations at one of the following target residues: Asp^{438}, Ser^{442}, Ile^{444}, Glu^{457}, Val^{471}, Ala^{472}, Gly^{473}, Glu^{481}, and Arg^{538}. These residues are located in the C-domain within a 4-Å radius from the binding site of *n*-decanol in the cleft (see Fig. 7, anesthetics in *black*). Mutations with amino acids having amphipathic side chains, such as W and Y, might change the luciferase sensitivity to anesthetics, thus critically testing our theoretical predictions.

Volatile anesthetics, in general, are low-affinity agents (12). They can associate with different regions of a protein, having different effects on protein functions. In the case of luciferase, above-unity Hill numbers are often found for various anesthetics, suggesting that these drugs interact with multiple sites in luciferase. The inhibition concentration of volatile anesthetics is typically in the hundred-micromolar to millimolar range (44). Hence, all sites predicted by docking in Fig. 6 are possible sites for anesthetic interaction, but they are not necessarily equally important to the inhibition of luciferase function, as will be discussed below in their different effects on the functionally important slow modes of motions. Because the location of the soaked bromoform molecules in the x-ray structure is adjacent to the luciferin binding area (2), it has been postulated that anesthetics compete with substrates for the same site. Other experimental data, however, suggested that volatile anesthetics and alcohols inhibited luciferase noncompetitively (9,44,45). It was also suggested in these studies that anesthetics interacted with luciferase nonspecifically and caused destabilization of luciferase in the absence of Mg-ATP. An opposite effect was observed later in the presence of Mg-ATP (14). In our docking studies, if the oxyluciferin was artificially removed from the closed structure and its binding pocket was searched again using AutoDock, 95% occupancy was found at the same oxyluciferin site. The binding energy for oxyluciferin is 1.6 kcal/mol lower than *n*-decanol at the same site. Thus, even with very potent anesthetics like *n*-decanol, the affinity ratio is 14 times in favor of oxyluciferin. Halothane would be at least three orders of magnitude less competitive than oxyluciferin for the substrate biding site. In any case, it

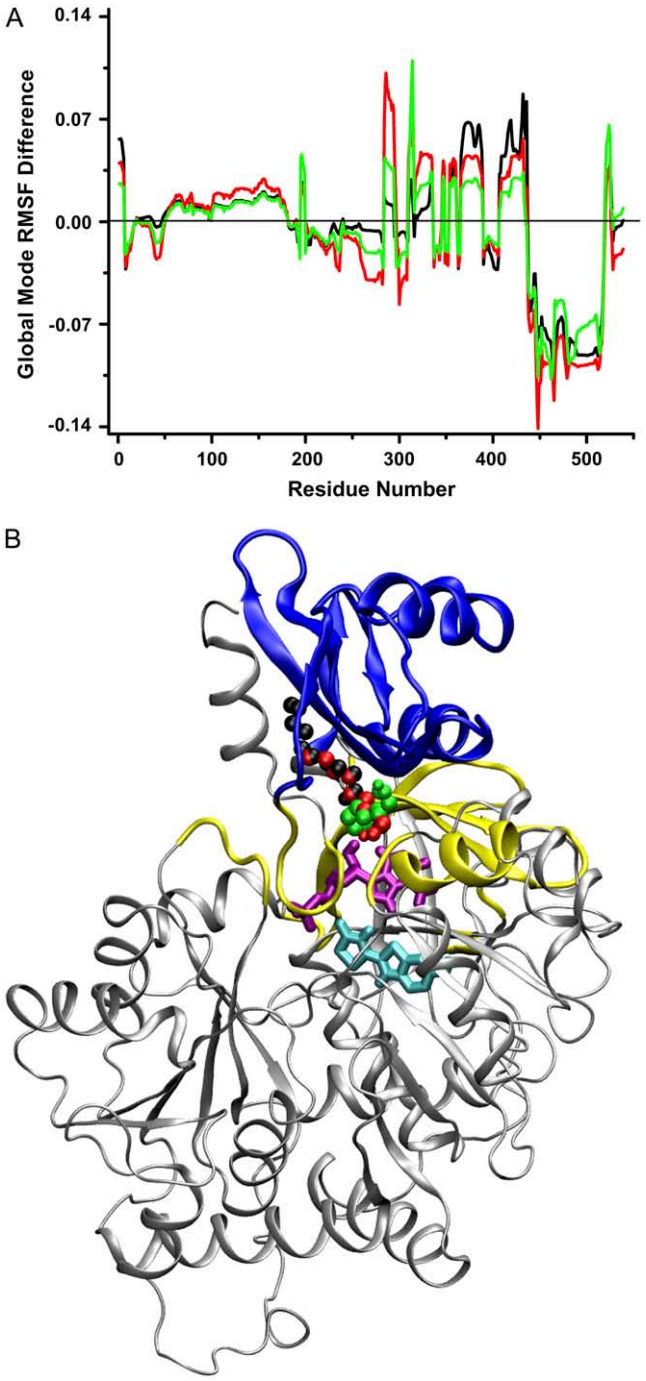

FIGURE 7 Differences of the RMSF, $\mathrm{sqrt}\langle\Delta R^2\rangle_{(\mathrm{protein\ +\ decanol})} - \mathrm{sqrt}\langle\Delta R^2\rangle_{(\mathrm{protein})}$, driven by the global GNM modes between the closed conformations with and without the docked *n*-decanol molecules. (*A*) Differences of RMSF induced by *n*-decanol molecules in three slightly different orientations at the cleft region of luciferase. Line colors in *A* match the colors of *n*-decanol molecules shown in *B*. Also in *B*, AMP and oxyluciferin are marked in pink and cyan, respectively. The regions with RMSF changes exceeding ±0.04 units under the influence of the anesthetic nodes are highlighted in yellow and blue, respectively.

seems unlikely that the inhibition of luciferase by a very diverse range of anesthetic molecules can result from their competition with the native substrates or products. It is thus worth exploring other possible mechanisms of anesthetic action on luciferase. As discussed in the following section, the anesthetic modulation of the global dynamics seems highly relevant to the anesthetic-induced inhibition of luciferase.

Dynamics changes upon anesthetic binding

Although the conventional all-atom molecular dynamics (MD) simulations of protein systems with docked anesthetics can provide detailed information about anesthetic-protein interaction (17,40), the current computational timescale of MD simulations is often not long enough to directly reveal anesthetic modulation on functionally relevant dynamics. In contrast, GNM and ANM analyses can effectively capture the anesthetic effects on global motion. By perturbing the protein backbone network with additional nodes to represent the docked anesthetics, we found that the presence of halothane or *n*-decanol in different regions of luciferase had distinctively different impacts on the protein global dynamics. Fig. 7 illustrates the changes in luciferase fluctuations in the presence and absence of *n*-decanol in the cleft region of the closed conformation. An analogous fluctuation profile for halothane (Fig. 1S in the Supplementary Material) is very similar in shape but shows smaller amplitude. This finding emphasizes the similarity in the mechanism of action exerted by the different anesthetic molecules. At the same time, the smaller amplitude of the effect by halothane is consistent with halothane's lower anesthetic potency compared to *n*-decanol. In the global mode, which directly relates to the conformational transitions between the open and closed states as discussed earlier in this article, there is a profound reduction in flexibility in almost all of the C-domain (as large as ~20% by comparing the amplitudes in Figs. 2 and 7).

This is consistent with the experimental finding that anesthetics stabilize the closed conformation in the presence of Mg-ATP (14). The stabilization of C-domain in the product-bound conformation can reduce the enzyme turnover, leading to apparent inhibition. Other noticeable changes when anesthetics bind to the cleft region are the moderate increase in the flexibility of the residues from T^{292} to D^{438} that are in contact with AMP (highlighted in *yellow* in Fig. 7 *B*). Moreover, the dynamics changes are fairly sensitive to the fine detail of the *n*-decanol position or orientation in the cleft. The presence of *n*-decanol in the cleft region also affects the all-mode cross correlation distribution, as shown in Fig. 3S in the online Supplementary Material. Particularly interesting changes in the correlation patterns can be seen in the L2 loop and the interdomain linker.

In sharp contrast, the perturbation to the global dynamics is much smaller when halothane or *n*-decanol molecules were placed in other plausible binding sites revealed by the docking, including the binding sites for oxyluciferin and AMP (Fig. 8). *N*-decanol docked at the oxyluciferin site can only produce local changes in those residues in direct contact with the anesthetic. It is also worth noting that the slowest GNM mode is virtually insensitive to the presence or absence of anesthetics at the lowest energy halothane binding site in the A subdomain or the bromoform-binding sites (see Fig. 1S in the Supplementary Material), suggesting that the high affinity anesthetic binding sites such as those revealed by soaking open-conformation crystals in saturated anesthetic solutions are not necessarily the functionally important sites for anesthetic action. Therefore, the region where anesthetics can impose the most profound dynamical effect is at the cleft—the interface between the N- and C-domains of luciferase. The mode of action is the anesthetic-induced reduction of global dynamics of the functional C-domain.

It is important to put the results in Figs. 2 and 3 and those in Figs. 7 and 8 into perspective with regard to each other. By the normal mode analysis of the experimental structures in two important functional conformations, we have established a link between the slow-mode dynamics and the enzymatic function. Most importantly, we have demonstrated that the first few slow modes can account for the tendency of the conformational transition from the open to the closed structures (Fig. 3). This, combined with the mutagenesis data by others about the role of cleft-facing residues in enzymatic activities, suggests that the slow modes of motion of the C-domain relative to the N-domain make the predominant contribution to the luciferase enzymatic function. Thus, it can be inferred that the profound anesthetic modulations among the slowest GNM and ANM modes, particularly the significant reduction of the C-domain movement relative to the N-domain (Fig. 7), suggest that the anesthetic action on this protein producing the apparent inhibition of enzymatic activity is through the modulation of the protein global dynamics.

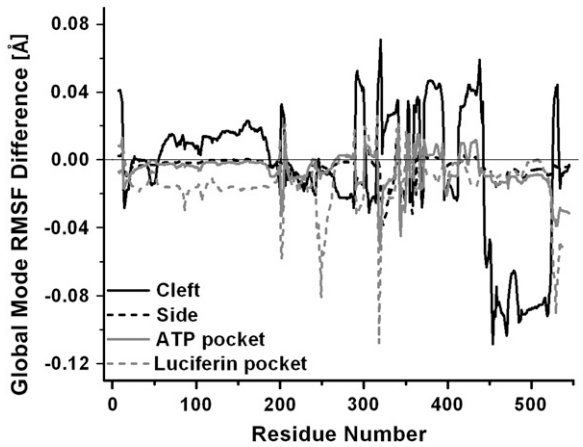

FIGURE 8 Summary of the RMSF differences induced by *n*-decanol molecules docked at different regions of luciferase. The calculation of RMSF difference induced by the individual *n*-decanol is the same as described in the Fig. 7 legend. Each curve represents an average of RMSF differences contributed by a cluster of *n*-decanol molecules in each specific region.

Despite the fact that most of the C-domain exhibits a reduced slow-mode motion when anesthetics interact with the cleft region, a significant flexibility increase in loop L2 (residues 526–533), which is a signature loop in the C-domain, is noticeable. A similar flexibility increase is also found from residues 292 to 302 and from 318 to 333. These residues are located at the interface of the C- and N-domains and near the ATP binding site. Lys^{529} in 1BA3 (homolog Lys^{531} in 2D1R) in loop L2 is a conserved residue of the acyl-adenylate-forming enzyme superfamily. Mutation experiments (20,46) suggested that Lys^{529} is critical for effective substrate orientation and provides the polar interactions to facilitate adenylate production. Substitution of Lys^{529} to other amino acids was found to result in over 100- to 1000-fold reduction in enzymatic activities (20). Thus, it is highly likely that the slackened structural characteristics of loop L2 at the interface of the N- and C-domains and the overall mobility of the C-domain are the result of evolution for this superfamily of enzymes to accommodate the need for the clamping and rotation motion of the C-domain relative to the N-domain to accomplish their biological functions. The anesthetic-induced changes in the slow-mode dynamics of Lys^{529} and its adjacent residues can affect the interaction of these residues with ATP. This, combined with the overall reduction in C-domain global mode motion, may underlie the apparent inhibition of the enzymatic activities.

The potential impact on higher frequency motions (up to mode 20) due to the presence of anesthetics in the cleft region was also examined. We found only scattered and local changes in fluctuations of loops and segments of subdomains A and B, as summarized in Fig. 2S in the Supplementary Material. The eigenvalue distribution is not significantly affected. The largest changes (eigenvalue increase) occur in modes 3 and 4, consistent with the shapes of these modes (see Fig. 5) that exhibit high fluctuations of the linker (mode 3) and moderate fluctuations of loops L1 and L2 (mode 4). These modes are therefore directly affected by the ligand located in the cleft. It is clear that only in the global mode is the C domain fluctuation affected significantly and non-locally by the presence of the anesthetic in the cleft region, leading to a profound impact on luciferase's function.

Finally, to confirm that the intrinsic dynamics pattern and anesthetic-induced dynamics changes observed in this study are not an artificial consequence of the coarse graining in GNM and ANM, we have employed a different variant of elastic network models to include in the calculation all heavy atoms in anesthetics and protein, including the side chains. The so-called rotational-translational blocks were used to simplify the Hessian matrix (32,47). Adopting the method implemented in *elNémo* (http://www.igs.cnrs-mrs.fr/elnemo/) (48), we calculated and compared the slowest normal modes for both *n*-decanol-free and *n*-decanol-bound luciferase in the closed conformation using all heavy atoms. The default cutoff radius was used. The *n*-decanol molecule was located in the cleft area in the locus and orientation corresponding to that marked in black in Fig. 7. The eigenvalue-weighted average of the first three modes, which corresponds to the GNM global mode, revealed a similar pattern of change in dynamics, validating the one-node-per-residue coarse-graining approach for analyzing slow dynamics.

In summary, our results confirm that as the luciferase transforms from the substrate-free to the product-bound state, the protein C-domain engages in a sequence of movements, including clamping, rotating, and rocking. The slow modes of collective C-domain motion dominate the large conformational change between two functional states. Although anesthetics can access many different regions, grooves, or pockets in luciferase, including luciferin and ATP binding sites, the anesthetics at the interface of N- and C-domains have the most profound impact on the global dynamics of the protein. The concerted C-domain movement, intimately coupled to the enzymatic activity, is shown to be highly susceptible to anesthetic modulations. Anesthetic-induced dynamics changes, most notably the reduced motion of the overall C-domain and altered flexibility in some of the residues adjacent to the ATP binding site, would most likely change the normal function of the protein and show up as an epiphenomenon of an inhibition. The results presented in this study reinforced our early viewpoint (17) that the functionally significant changes in dynamics at various sites of a protein are governed predominantly by the protein's intrinsic susceptibility to the environment-controlled dynamical modulations. As long as the modulators (anesthetics) are present, the global change in dynamics will occur and will be additive, leading to the corresponding functional changes. Such a viewpoint offers a unitary explanation for different anesthetic action on a diverse range of proteins and can be systematically tested in future studies on other proteins.

SUPPLEMENTARY MATERIAL

To view all of the supplemental files associated with this article, visit www.biophysj.org.

The authors thank Dr. A. J. Rader and Prof. I. Bahar for invaluable discussions on the use of GNM and ANM programs and Dr. A. S. Saladino for initial technical assistance.

This research was supported in part by grants from the National Institutes of Health (R01GM066358 and R01GM056257 to P.T. and R37GM049202 to Y.X.).

REFERENCES

1. Conti, E., T. Stachelhaus, M. A. Marahiel, and P. Brick. 1997. Structural basis for the activation of phenylalanine in the non-ribosomal biosynthesis of gramicidin S. *EMBO J.* 16:4174–4183.
2. Franks, N. P., A. Jenkins, E. Conti, W. R. Lieb, and P. Brick. 1998. Structural basis for the inhibition of firefly luciferase by a general anesthetic. *Biophys. J.* 75:2205–2211.
3. May, J. J., N. Kessler, M. A. Marahiel, and M. T. Stubbs. 2002. Crystal structure of DhbE, an archetype for aryl acid activating domains of

modular nonribosomal peptide synthetases. *Proc. Natl. Acad. Sci. USA.* 99:12120–12125.

4. Gulick, A. M., X. Lu, and D. Dunaway-Mariano. 2004. Crystal structure of 4-chlorobenzoate:CoA ligase/synthetase in the unliganded and aryl substrate-bound states. *Biochemistry.* 43:8670–8679.
5. Gulick, A. M., V. J. Starai, A. R. Horswill, K. M. Homick, and J. C. Escalante-Semerena. 2003. The 1.75 A crystal structure of acetyl-CoA synthetase bound to adenosine-5′-propylphosphate and coenzyme A. *Biochemistry.* 42:2866–2873.
6. Nakatsu, T., S. Ichiyama, J. Hiratake, A. Saldanha, N. Kobashi, K. Sakata, and H. Kato. 2006. Structural basis for the spectral difference in luciferase bioluminescence. *Nature.* 440:372–376.
7. Oba, Y., M. Ojika, and S. Inouye. 2003. Firefly luciferase is a bifunctional enzyme: ATP-dependent monooxygenase and a long chain fatty acyl-CoA synthetase. *FEBS Lett.* 540:251–254.
8. Fontes, R., B. Ortiz, A. de Diego, A. Sillero, and M. A. Gunther Sillero. 1998. Dehydroluciferyl-AMP is the main intermediate in the luciferin dependent synthesis of Ap4A catalyzed by firefly luciferase. *FEBS Lett.* 438:190–194.
9. Ueda, I. 1965. Effects of diethyl ether and halothane on firefly luciferin bioluminescence. *Anesthesiology.* 26:603–606.
10. Franks, N. P., and W. R. Lieb. 1984. Do general anaesthetics act by competitive binding to specific receptors? *Nature.* 310:599–601.
11. Franks, N. P., and W. R. Lieb. 2004. Seeing the light: protein theories of general anesthesia. 1984. *Anesthesiology.* 101:235–237.
12. Campagna, J. A., K. W. Miller, and S. A. Forman. 2003. Mechanisms of actions of inhaled anesthetics. *N. Engl. J. Med.* 348:2110–2124.
13. Ueda, I., H. Matsuki, H. Kamaya, and P. R. Krishna. 1999. Does pressure antagonize anesthesia? Opposite effects on specific and nonspecific inhibitors of firefly luciferase. *Biophys. J.* 76:483–488.
14. Eckenhoff, R. G., J. W. Tanner, and P. A. Liebman. 2001. Cooperative binding of inhaled anesthetics and ATP to firefly luciferase. *Proteins.* 42:436–441.
15. Ueda, I. 2001. Molecular mechanisms of anesthesia. *Keio J. Med.* 50:20–25.
16. Takehara, K., H. Kamaya, and I. Ueda. 2005. Inhibition of firefly luciferase by alkane analogues. *Biochim. Biophys. Acta.* 1721:124–129.
17. Tang, P., and Y. Xu. 2002. Large-scale molecular dynamics simulations of general anesthetic effects on the ion channel in the fully hydrated membrane: the implication of molecular mechanisms of general anesthesia. *Proc. Natl. Acad. Sci. USA.* 99:16035–16040.
18. Conti, E., N. P. Franks, and P. Brick. 1996. Crystal structure of firefly luciferase throws light on a superfamily of adenylate-forming enzymes. *Structure.* 4:287–298.
19. Zako, T., K. Ayabe, T. Aburatani, N. Kamiya, A. Kitayama, H. Ueda, and T. Nagamune. 2003. Luminescent and substrate binding activities of firefly luciferase N-terminal domain. *Biochim. Biophys. Acta.* 1649:183–189.
20. Branchini, B. R., M. H. Murtiashaw, R. A. Magyar, and S. M. Anderson. 2000. The role of lysine 529, a conserved residue of the acyl-adenylate-forming enzyme superfamily, in firefly luciferase. *Biochemistry.* 39:5433–5440.
21. Tirion, M. M. 1996. Large amplitude elastic motions in proteins from a single-parameter, atomic analysis. *Phys. Rev. Lett.* 77:1905–1908.
22. Hinsen, K. 1998. Analysis of domain motions by approximate normal mode calculations. *Proteins.* 33:417–429.
23. Bahar, I., A. R. Atilgan, and B. Erman. 1997. Direct evaluation of thermal fluctuations in proteins using a single-parameter harmonic potential. *Fold. Des.* 2:173–181.
24. Atilgan, A. R., S. R. Durell, R. L. Jernigan, M. C. Demirel, O. Keskin, and I. Bahar. 2001. Anisotropy of fluctuation dynamics of proteins with an elastic network model. *Biophys. J.* 80:505–515.
25. Bahar, I., and A. J. Rader. 2005. Coarse-grained normal mode analysis in structural biology. *Curr. Opin. Struct. Biol.* 15:586–592.
26. Ma, J. 2005. Usefulness and limitations of normal mode analysis in modeling dynamics of biomolecular complexes. *Structure.* 13:373–380.
27. Fiser, A., R. K. Do, and A. Sali. 2000. Modeling of loops in protein structures. *Protein Sci.* 9:1753–1773.
28. Humphrey, W., A. Dalke, and K. Schulten. 1996. VMD: Visual Molecular Dynamics. *J. Mol. Graph.* 14:33–38, 27–28.
29. Bahar, I., B. Erman, T. Haliloglu, and R. L. Jernigan. 1997. Efficient characterization of collective motions and interresidue correlations in proteins by low-resolution simulations. *Biochemistry.* 36:13512–13523.
30. Rader, A. J., C. Chennubhotla, L. W. Yang, and I. Bahar. 2006. The Gaussian Network Model: Theory and Applications. CRC Press, Taylor & Francis Group, Baca Raton, FL.
31. Zheng, W., B. R. Brooks, S. Doniach, and D. Thirumalai. 2005. Network of dynamically important residues in the open/closed transition in polymerases is strongly conserved. *Structure.* 13:565–577.
32. Tama, F., and Y. H. Sanejouand. 2001. Conformational change of proteins arising from normal mode calculations. *Protein Eng.* 14:1–6.
33. Shrivastava, I. H., and I. Bahar. 2006. Common mechanism of pore opening shared by five different potassium channels. *Biophys. J.* 90: 3929–3940.
34. Yang, L. W., and I. Bahar. 2005. Coupling between catalytic site and collective dynamics: a requirement for mechanochemical activity of enzymes. *Structure.* 13:893–904.
35. Yang, L. W., X. Liu, C. J. Jursa, M. Holliman, A. J. Rader, H. A. Karimi, and I. Bahar. 2005. iGNM: a database of protein functional motions based on Gaussian network model. *Bioinformatics.* 21:2978–2987.
36. Morris, G. M., D. S. Goodsell, R. S. Halliday, R. Huey, W. E. Hart, R. K. Belew, and A. J. Olson. 1998. Automated docking using a Lamarckian genetic algorithm and an empirical binding free energy function. *J. Comput. Chem.* 19:1639–1662.
37. Tang, P., I. Zubryzcki, and Y. Xu. 2001. Ab initio calculation of structures and properties of halogenated general anesthetics: halothane and sevoflurane. *J. Comput. Chem.* 22:436–444.
38. Liu, Z. W., Y. Xu, A. C. Saladino, T. Wymore, and P. Tang. 2004. Parametrization of 2-bromo-2-chloro-1,1,1-trifluoroethane (halothane) and hexafluoroethane for nonbonded interactions. *J. Phys. Chem. A.* 108:781–786.
39. Frisch, M. J., G. W. Trucks, H. B. Schlegel, G. E. Scuseria, M. A. Robb, J. R. Cheeseman, J. A. Montgomery Jr., T. Vreven, K. N. Kudin, J. C. Burant, J. M. Millam, S. S. Iyengar, J. Tomasi, and others. 1998. Gaussian 98 (Revision A5). Gaussian, Inc., Pittsburgh, PA.
40. Yonkunas, M. J., Y. Xu, and P. Tang. 2005. Anesthetic interaction with ketosteroid isomerase: insights from molecular dynamics simulations. *Biophys. J.* 89:2350–2356.
41. Baldwin, T. O. 1996. Firefly luciferase: the structure is known, but the mystery remains. *Structure.* 4:223–228.
42. Moss, G. W., N. P. Franks, and W. R. Lieb. 1991. Modulation of the general anesthetic sensitivity of a protein: a transition between two forms of firefly luciferase. *Proc. Natl. Acad. Sci. USA.* 88:134–138.
43. Chiara, D. C., L. J. Dangott, R. G. Eckenhoff, and J. B. Cohen. 2003. Identification of nicotinic acetylcholine receptor amino acids photolabeled by the volatile anesthetic halothane. *Biochemistry.* 42:13457–13467.
44. Ueda, I., and A. Suzuki. 1998. Irreversible phase transition of firefly luciferase: contrasting effects of volatile anesthetics and myristic acid. *Biochim. Biophys. Acta.* 1380:313–319.
45. Ueda, I., and A. Suzuki. 1998. Is there a specific receptor for anesthetics? Contrary effects of alcohols and fatty acids on phase transition and bioluminescence of firefly luciferase. *Biophys. J.* 75:1052–1057.
46. Branchini, B. R., R. A. Magyar, M. H. Murtiashaw, S. M. Anderson, L. C. Helgerson, and M. Zimmer. 1999. Site-directed mutagenesis of firefly luciferase active site amino acids: a proposed model for bioluminescence color. *Biochemistry.* 38:13223–13230.
47. Delarue, M., and Y. H. Sanejouand. 2002. Simplified normal mode analysis of conformational transitions in DNA-dependent polymerases: the elastic network model. *J. Mol. Biol.* 320:1011–1024.
48. Suhre, K., and Y. H. Sanejouand. 2004. ElNemo: a normal mode web server for protein movement analysis and the generation of templates for molecular replacement. *Nucleic Acids Res.* 32:W610–W614.